JOURNAL OF IMAGING SCIENCE AND TECHNOLOGY • Volume 42, Number 5, September/October 1998

The Mechanism of Cyanine Sensitizing Dye Adsorption on AgBr Crystals

Hiroaki Ando, Noriko Ohara and Haruhiko Masutomi

Konica Corporation, Hino, Tokyo, Japan

Time evolution of the adsorption of cyanine sensitizing dyes onto silver halide crystals was investigated. Observing the adsorption process in this method was found to be useful in determining dye adsorption mechanisms and their rate determining steps, in revealing how the N-substituents of cyanine dyes change the adsorption, and in exploring the relationship between rate determining steps and the states of the dyes adsorbed.

Journal of Imaging Science and Technology 42: 427–433 (1998)

Introduction

Because spectral sensitization extends the sensitivity of silver halide grains from the relatively shorter wavelengths of visible light to the full visible spectrum, it is essential to color photography. As the spectral sensitization depends on the adsorption of sensitizing dyes onto silver halide grains, many researchers have reviewed this crucial process.[1] In addition, a number of specialized studies have been reported. Tani, Suzumoto and Ohzeki studied the immigration of photoelectrons from sensitizing dyes to AgBr grains.[2] Maskasky obtained large J-aggregates of sensitizing dyes on silver halide crystals, observed their low-temperature luminescence, and examined the arrangement of sensitizing dyes in these J-aggregates.[3] Saijyo et al, observed smaller J-aggregates of sensitizing dyes using ACFEM.[4] Kawasaki and Ishii observed J-aggregates of sensitizing dyes on silver halide monolayers using STM.[5] Asanuma and Tani studied the phenomenon of sensitizing dye desorption from J-aggregates on silver halide grains, reporting that desorption is affected by the size of the J-aggregate.[6] Mifune reported on the selectivity of the adsorption of sensitizing dyes onto silver halide grains of various iodine contents and crystal habits.[7] These studies reflect the particular interest of many researchers in the adsorption state of the J-aggregates of sensitizing dyes.

Sensitizing dyes are usually added into emulsions as a solution in a solvent or a dispersion in a dispersion medium and are adsorbed onto silver halide grains, where they form J-aggregates. Although many articles have reported on the equilibrium state of adsorption, very little is known about the adsorption process itself, and so we directed our attention to that process. By using novel apparatus that allowed more precise observation, we obtained useful data regarding the mechanism of dye adsorption. In some cases, we were able to determine the value of the activation energy of dye adsorption as a reaction between sensitizing dye monomers and the silver halide grain surface.

Experimental

Our experimental procedures were designed to study the mechanism of cyanine sensitizing dye adsorption on AgBr crystals. We prepared a AgBr, octahedral grain emulsion in a gelatin solution, with an average grain size of 1.1 mm. Using a KNO_3 aqueous solution, ionic conductivity was tuned to 10 mS/cm (40°C).

We studied the adsorption of three variations of thiacarbocyanine sensitizing dye (Fig. 1): Dye 1, 3,3'-bis-(3-sulfopropyl)-5,5'-dichloro-9-ethyl-thiacarbocyanine, an anionic dye; Dye 2, 3-ethyl,3'-(3-sulfopropyl) -5,5'-dichloro-9-ethyl-thiacarbocyanine, a betainic dye; and Dye 3, 3,3'-diethyl-5,5'-dichloro-9-ethyl-thiacarbocyanine, a cationic dye. In the anionic Dye 1, both of the substituents, R1 and R2, had a negative charge, so the total charge of the anionic dye molecule was negative. In the betainic Dye 2, one substituent was negative and the other was neutral, but because of the positive charge of the nitrogen atom above R1, the total charge was neutral. And in the cationic Dye 3, both substituents were neutral, but again because of the positive charge of the nitrogen atom above R1, the total charge was positive.

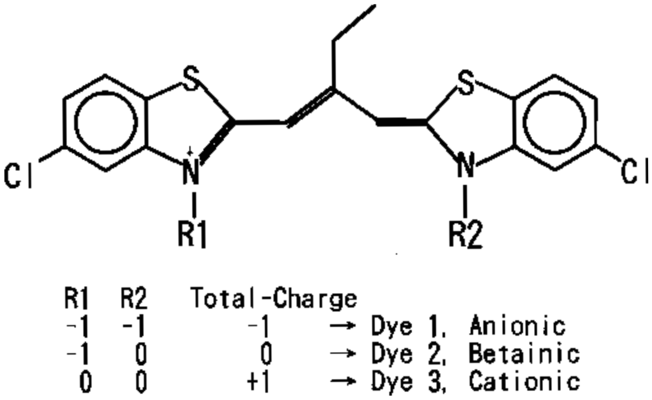

R1	R2	Total-Charge	
-1	-1	-1	→ Dye 1, Anionic
-1	0	0	→ Dye 2, Betainic
0	0	+1	→ Dye 3, Cationic

Figure 1. Cyanine dyes studied.

Original manuscript received April 2, 1998

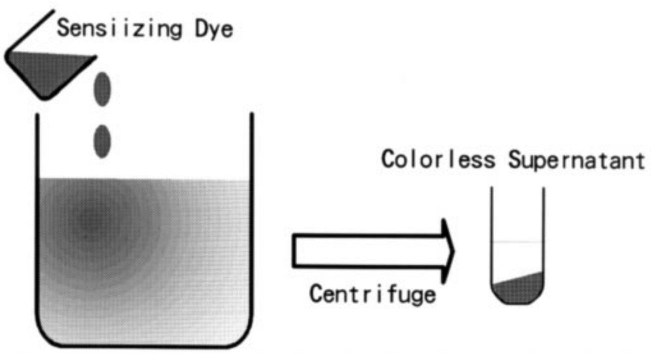

Scheme 1. *Inapplicability of Centrifuging.* Centrifuging an emulsion takes at least 20 to 30 s, by which time dye adsorption is already complete, making centrifuging inapplicable to the analysis of the dye adsorption process.

Organic solvents are often used to dissolve sensitizing dyes for addition to emulsions for spectral sensitization. But mixing an organic solvent and water is an exothermic reaction, and the adsorption process is greatly affected by the rise of emulsion temperature. In addition, because of the difference in solubility of a dye in water and a dye in an organic solvent, deposition of the sensitizing dye from the organic solvent occurs just after the addition of sensitizing dye. These phenomena would have made it difficult to observe the dye adsorption process precisely if we had used an organic solvent, so we used dispersion instead. We prepared our dispersions by dispersing a sensitizing dye powder in water, adding gelatin and KNO_3 in appropriate concentrations to the dispersion, bringing the dispersion up to the temperature of the emulsion, and, finally, adding it to the emulsion. This eliminated the influence of exothermic reactions and the deposition of the sensitizing dye.

Although amounts of adsorbed dyes are commonly calculated from the amount of dye in the supernatant of a centrifuged emulsion (Scheme 1), we found it impossible to determine the time dependency of the amount of dye adsorbed with this method. Centrifuging required 20 to 30 s to separate the supernatant from the emulsion, but we found that, even at the relatively high coverage of 80%, adsorption was completed so quickly that the supernatant was colorless. This meant that adsorption of the sensitizing dye was too rapid for the application of a centrifuge technique.

Therefore, we developed a technique suited to the speed of the adsorption process being studied. We used in situ measurements of reflection spectra and a function based on the Kubelka–Munk equation to estimate cumulative amounts of dye adsorbed during the actual process of adsorption. To do this, we connected optical fiber to the reaction vessel and acquired the reflection spectra in situ (Fig. 2). We used a spectrometer equipped with a diode-array-type detector and a xenon lamp, and we measured the spectra at 2 s intervals. We chose a 2 s interval because it took approximately 1 s for the emulsion and dye dispersion to mix completely, so that measurements at shorter intervals would have been affected by mixing conditions. Likewise, our measurements were conducted at 40 to 50°C, a range of temperature high enough to allow homogeneous mixing and adsorption of the sensitizing dye, but low enough to allow mixing to complete before adsorption was far advanced.

Results and Discussion

Our study had three points of interest: first, the implications of our observations of the dye adsorption process regarding dye adsorption mechanisms and their rate determining steps; second, the effect on the dye adsorption mechanism of varying the N-substituents of dye molecules; and, third, the relationship between rate determining steps and the states of dyes adsorbed.

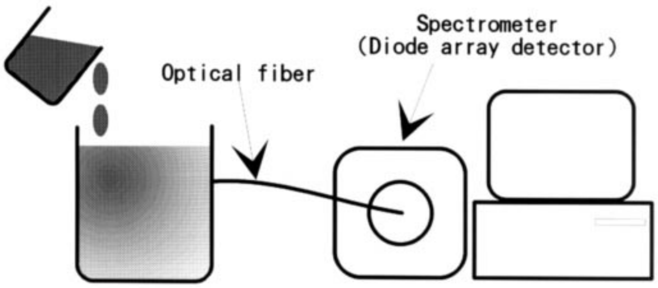

Figure 2. In-situ acquisition of reflection specta. Spectrometer: MCPD-1000 (Otska Electronics Co., Ltd., Osaka, Japan)

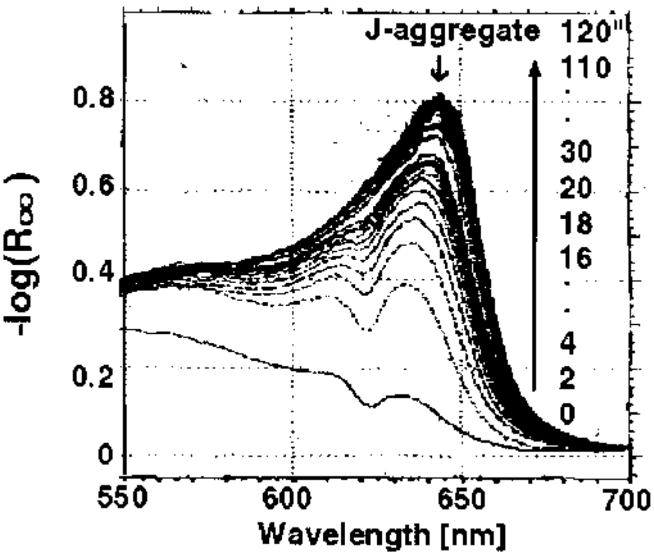

Figure 3. Time evolution of adsorption, Dye 1.

Observing the Dye Adsorption Process and Determining the Adsorption Mechanism and Rate Determining Step. Using just enough dye to achieve saturation coverage, we added the anionic Dye 1 to an emulsion containing 1.1 μm octahedral, AgBr crystals. Then, using the apparatus described above, we measured reflection spectra every 2 s and observed the progress of the sensitizing dye's adsorption on the surface of the crystals (Fig. 3). In the set of reflection spectra that resulted, the main peak, at 645-nm, emerged as soon as the sensitizing dye was added. This main peak was assigned to the J-aggregate of the dye on the crystals. Note that in the 560 to 570-nm region there was no large dye monomer peak and that only a very slight shoulder was noticeable.

Based on the Kubelka–Munk equation, the function $(1 - R_\infty)^2/2R_\infty$ (where R_∞ is the reflectivity) is known to increase proportionally to the relative amount of sensitizing dye adsorbed. By applying this function to the reflectivity of the J-aggregate peaks, we were able to calculate the cumulative amount of dye adsorbed at any point during the adsorption process (Fig. 4). Our data showed that adsorption initiates at a high rate and then falls continuously until saturation is reached.

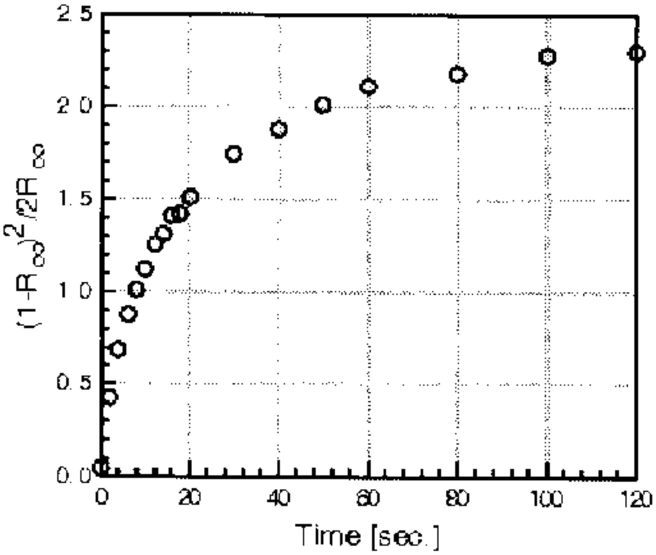

Figure 4. Relative amounts of dye adsorbed over time, Dye 1, at 45°C.

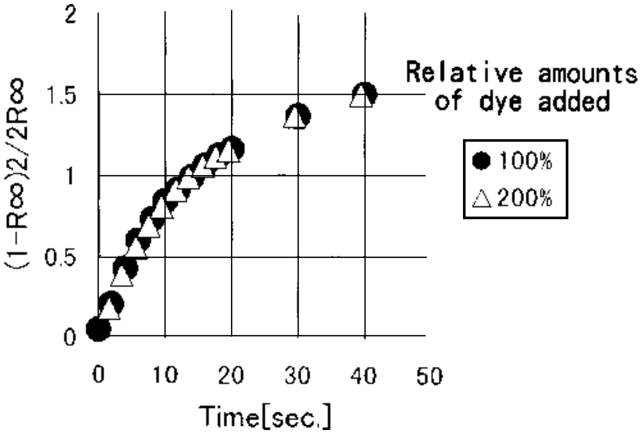

Figure 5. Adsorption rate unaffected by amount of dye added, Dye 1, at 41°C.

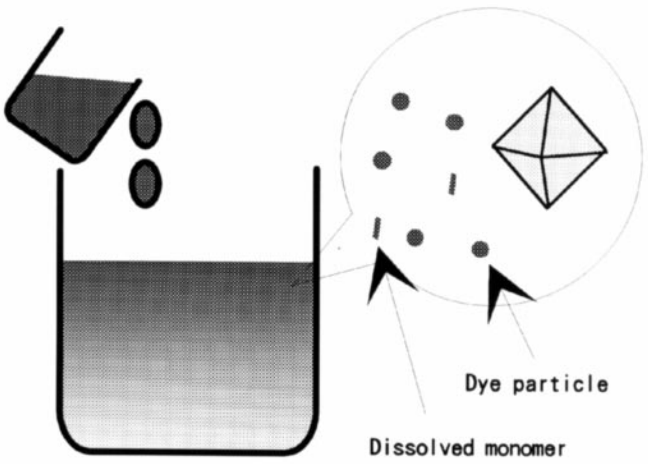

Figure 6. Low dye solubility in the presence of gelatin and KNO_3, Dye 1.

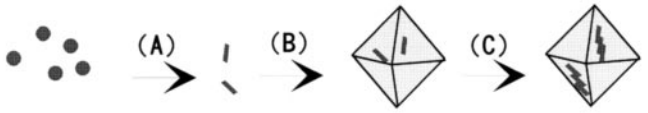

Scheme 2. *Three-step Adsorption Mechanism, Dye 1.* In Step A, dye particles dissolve; in Step B, dissolved monomers contact AgBr crystal surfaces and adsorb; and in Step C, the adsorbed monomers arrange into J-aggregates.

These data suggested three different mechanisms of dye adsorption: the adsorption rate could depend on the amount of unadsorbed sensitizing dye, on the number of vacant sites on the silver halide grains, or on both. To determine which was the case, we repeated the process but doubled the amount of sensitizing dye added (Fig. 5). The results clearly showed that the amount of dye added had no effect on the adsorption rate; rather, the adsorption rate appeared to depend on the number of vacant sites present on the AgBr crystals.

To explore why this might be so, we studied our dye dispersion. We found that solubility was very low (<3 mg/100 mL) in the presence of gelatin and KNO_3, allowing us to project that less than 5% of the total amount of Dye 1 added had dissolved, with the remainder taking the form of undissolved particles (Fig. 6). This suggested that the dye molecules in particles may not be able to adsorb directly onto the silver halide surface, but must first dissolve, explaining why the adsorption rate is not affected by the amount of dye added. If only dissolved monomers can adsorb on the surface, then adsorption depends on the opportunity for contact between the dissolved dye monomers and the vacant sites on the AgBr crystals. Because the supply of dissolved monomers is constantly being replenished, but the number of vacant sites is not, the dwindling number of vacant sites would account for the continuously falling adsorption rate.

This suggested a three-step dye adsorption mechanism in which (A) the dye particles dissolve into free monomers; (B) these free monomers adsorb onto the AgBr crystal grains; and (C) the adsorbed free monomers then arrange themselves into J-aggregates, which was observed in the spectrum (Scheme 2). The rate determining step here would clearly not be Step A, for, if it were, the adsorption rate would have been affected by the amount of dye added to the emulsion, which it was not. Nor would the rate determining step be Step C, for then a large monomer peak would have appeared in the reflection spectra, and no such monomer peak appeared. Thus, by elimination, Step B, in which the free monomers adsorb onto the AgBr crystal grains, appeared to be the rate determining step, and the adsorption rate here was most plausibly determined by the number of AgBr crystal sites vacant and thus able to accommodate dye adsorption.

To examine this idea further, we determined rate constant and activation energy in the following way: The total number of vacant sites on the AgBr crystals and the amount of dye needed to achieve saturation coverage are directly related, therefore dye adsorption can be described by this equation:

$$A = A_{sat} \times (1 - e^{-kt}), \tag{1}$$

where A is the amount of dye adsorbed and A_{sat} is the saturation amount, and both A and A_{sat} are substituted for by values determined from a function based on the Kubelka–Munk equation.

By plotting the logarithm of Eq. 1 against time, we obtained a straight line, confirming the equation's validity

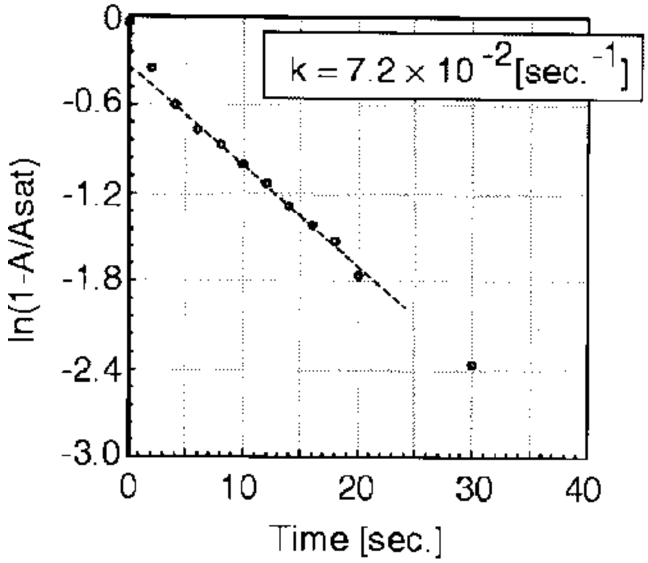

Figure 7. Adsorption rate well expressed as first-order kinetics, Dye 1.

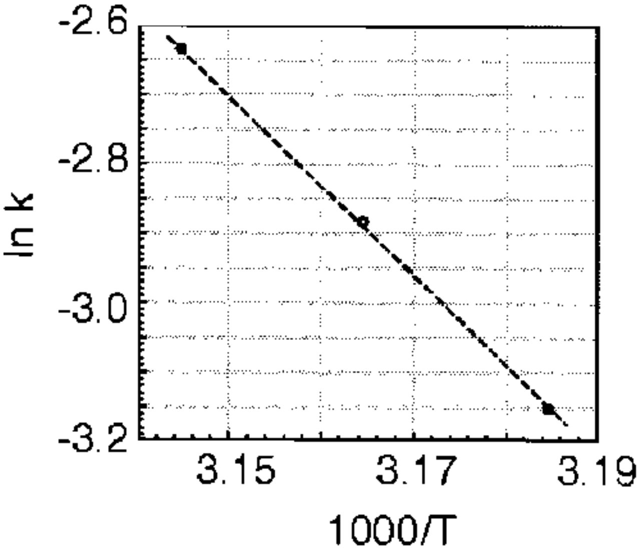

Figure 8. Determining activation energy, Dye 1.

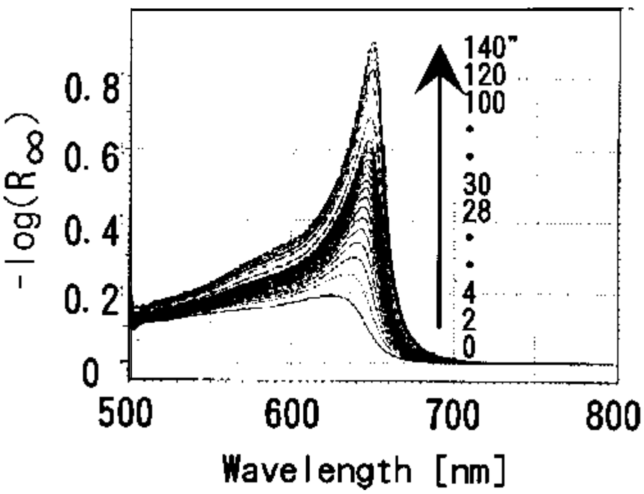

Figure 9. Time evolution of adsorption, Dye 2.

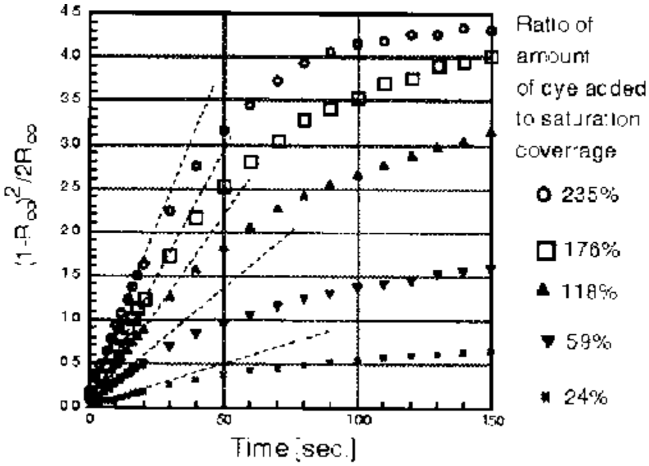

Figure 10. Adsorption rate affected by amount of dye added, Dye 2.

and indicating that the dye adsorption rate was of first-order kinetics (Fig. 7). From the slope, the value of the rate constant, k, equaled 7.2×10^{-2} s^{-1}. We then calculated activation energy by measuring the adsorption rates in the range of 41 to 45°C and then constructing an Arrhenius plot (Fig. 8). This plot gave a straight line resulting in an activation energy of 26 kcal/mol for Dye 1. Thus, observing the time evolution of the adsorption process proved useful in studying dye adsorption mechanisms and their rate determining steps.

Effects of Varying the N-Substituents of Dye Molecules. Our second focus was on the effects of varying the N-substituents of the dye molecules. As with the anionic dye, Dye 1, we measured reflection spectra during the adsorption of the betainic dye, Dye 2, and, as with Dye 1, the J-aggregation peaks dominated the spectra (Fig. 9). Using the same function as with Dye 1, we plotted the relative amount of dye adsorbed against time, and found that, unlike Dye 1, the adsorption rate of Dye 2 did depend on the amount of dye added.

Expressed as a percentage against saturation coverage, when a larger amount of dye was added, the adsorption rate increased (Fig. 10). From the tangents of these plots, we calculated and plotted initial adsorption rates (Fig. 11), which resulted in a straight line indicating that the dye's initial adsorption rate is proportional to the amount of dye added.

From these observations, we considered two alternate mechanisms of adsorption for Dye 2 (Scheme 3). Mechanism A is identical to that proposed for Dye 1 (Scheme 2), i.e., by this mechanism, Dye 2 would not adsorb onto the AgBr crystals in particle form, but would dissolve and then adsorb in monomer form. However, because of Dye 2's low monomer solubility, the rate determining step here would be particle dissolution, with the adsorption rate depending on the available dye particle surface area. Thus, increasing the amount of dye added would raise the rate of adsorption. In Mechanism B, Dye 2 would adsorb onto the AgBr crystals in particle form. In this case, increasing the amount of dye added would increase the probability of dye–crystal contact, thus increasing the adsorption rate.

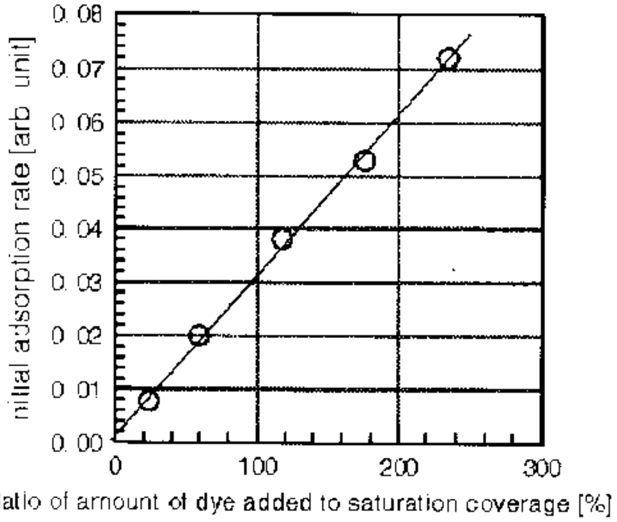

Figure 11. Initial adsorption proportional to amount of dye added, Dye 2.

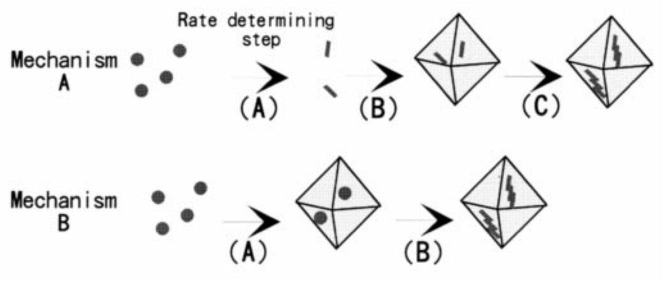

Scheme 3. *Alternate dye adsorption mechanisms, Dye 2.* Mechanism A is identical to that proposed for Dye 1 (Scheme 2), but the rate determining step for Dye 2 is Step A. In Mechanism B, in Step A, dye particles adsorb in particle form, and, in Step B, they arrange into J-aggregates; the rate determining step is Step A.

To determine which mechanism was more likely, we studied the adsorption rates of Dye 2 in emulsions in which we varied the AgBr crystal concentration by increasing the emulsion volume but maintained the same ratio of added dye to AgBr crystals. Our thinking was that if Mechanism B was operative, the adsorption rate could be expected to rise and fall with AgBr concentration because increasing and decreasing the AgBr concentration could be expected to likewise increase and decrease the incidents of dye particle–crystal contact. However, no such change in adsorption rate appeared (Fig. 12), making Mechanism A, in which monomers and not particles are adsorbed, the more likely adsorption mechanism.

As with Dye 1 and Dye 2, we measured the reflection spectra of the cationic dye, Dye 3. We found that, like Dye 2, the adsorption rate depended on the amount of dye added. But, unlike Dye 2, the initial adsorption rate was not proportional to the amount of dye added (Fig. 13). For example, when we doubled the amount of added dye, the initial adsorption rate nearly tripled. This leaves the adsorption mechanism of Dye 3 unclear. The increase of total surface area of the dye particles cannot account for the acceleration of the adsorption rate, and although the two mechanisms proposed for Dye 2 can be proposed here as well, neither can be eliminated.

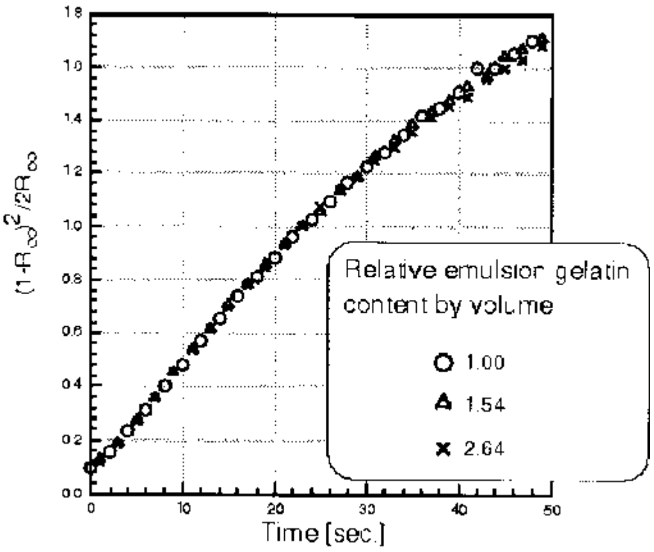

Figure 12. Adsorption rate unaffected by AgBr crystal concentration, Dye 2.

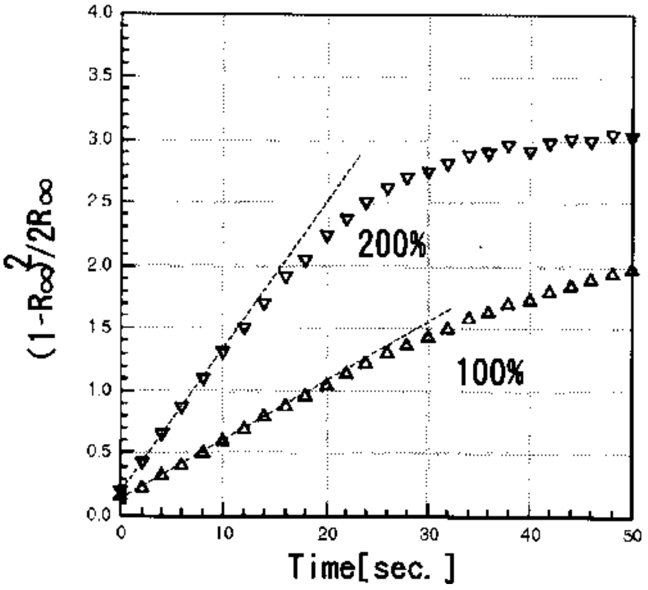

Figure 13. Adsorption rate affected by, but not proportional to, amount of dye added, Dye 3.

Thus, we found that varying the N-substituents of these three thiacarbocyanine dyes led to different mechanisms of adsorption. Comparing the solubility of these three dyes is difficult, but the spectra for each dye at the point at which half of the added dye has been adsorbed yields intriguing data (Fig. 14). The spectrum of Dye 1 differs greatly from those of Dyes 2 and 3. In the shorter wavelength region, there is a broad shoulder leading up to the J-aggregate peak that might be attributed to monomers that have dissolved and have not yet been adsorbed. Although this anionic dye's solubility is not very high, this distinct shoulder suggests that it is higher than that of the betainic and cationic dyes, which may help explain the apparent differences in the dyes' mechanisms of adsorption.

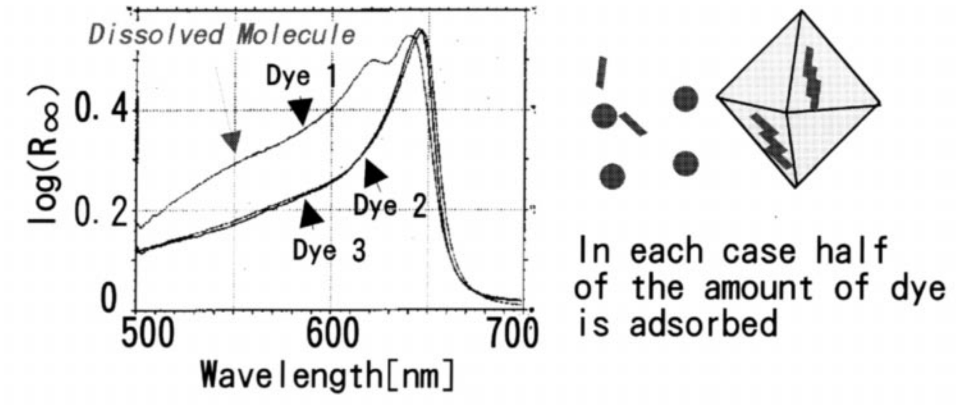

Figure 14. Mid-adsorption spectra indicative of solubility.

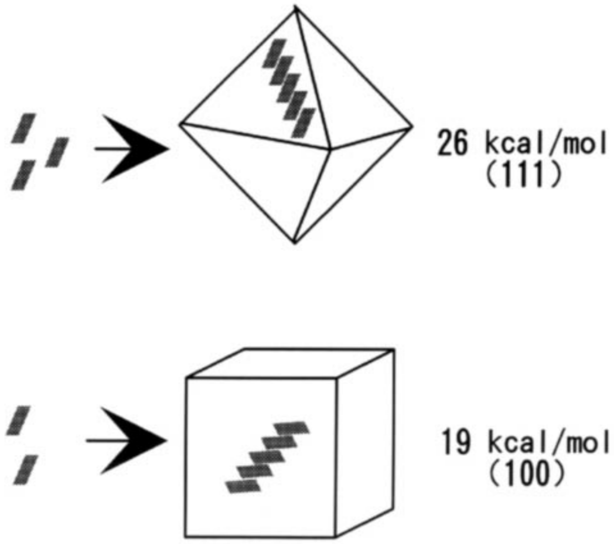

Figure 15. Activation energies vary with crystal habit, Dye 1.

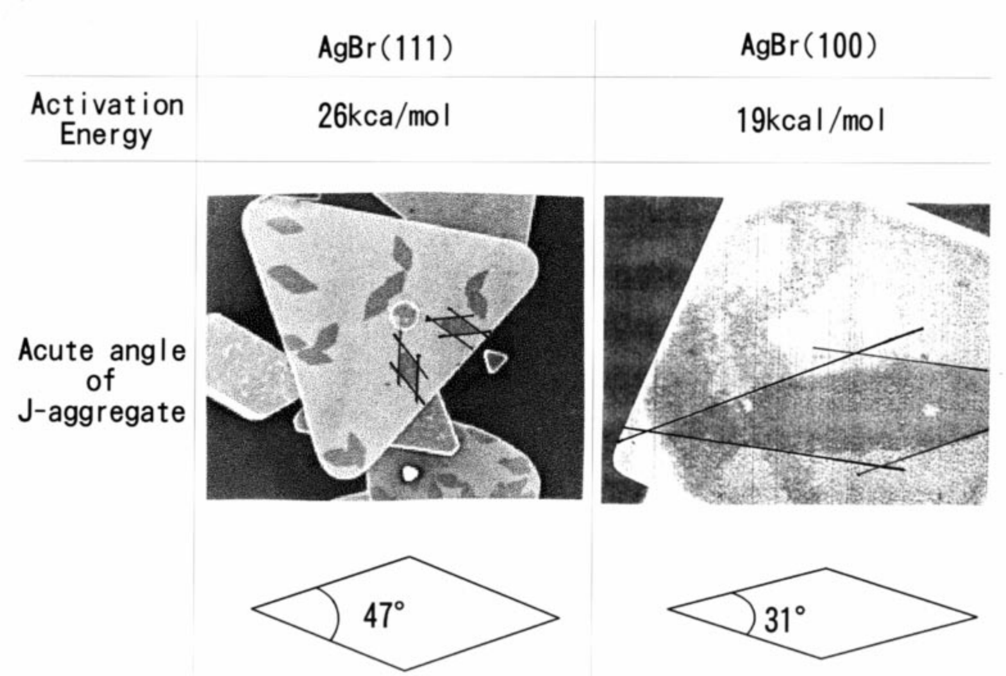

Figure 16. J-aggregate parallelogram angles vary with crystal habit, Dye 1.

Rate Determining Steps and the States of the Dyes Adsorbed. To explore the relationship between rate determining steps and the states of the adsorbed dyes, we turned to crystal habit. We had found the rate determining step of Dye 1 to be the adsorption of dye monomers onto the surface of the AgBr crystal grains, so that Dye 1's activation energies reflect the way in which the dye monomers adsorb onto the octahedral AgBr grain surfaces. We now measured Dye 1's adsorption rate onto AgBr cubic grains and calculated an activation energy of 19 kcal/mol, which was far lower than the 26 kcal/mol found with octahedral grains, indicating that activation energies vary with crystal habit (Fig. 15).

To see the effect of crystal habit, we used SEM imaging to observe J-aggregates (grown by the method proposed by Maskasky[3]) on the surfaces of both <111> and <100> grains (Fig. 16). In both cases, the J-aggregates clearly appear in parallelogram form, but the acute angles of these parallelograms differ. On the <111> surface, the acute angle is approximately 47°, while on the <100> surface, it is approximately 31°. Such differences may have important implications regarding the arrangement and conformation of the J-aggregates associated with these angles and, ultimately, on the relationship between rate determining steps and the states of the dyes adsorbed.

Conclusion

Our study of the process of sensitizing dye adsorption yielded valuable results. We learned that observing the adsorption process as it occurs can provide data useful in determining dye adsorption mechanisms and their rate determining steps, in revealing how the N-substituents of cyanine dyes alter the adsorption mechanisms involved, and in exploring the relationship between rate determining steps and the states of the dyes adsorbed.

Acknowledgment. We are very grateful to Mr. Yoshihiko Suda of Konica Corporation for his invaluable suggestions and encouragement.

References

1. For example, *The Theory of the Photographic Process*, 4th ed., T. H. James, Ed., Macmillan, New York, 1977, Chap. 9: *Photographic Sensitivity*, T. Tani, Oxford University Press, New York, 1995, Chap. 5, Sect. 5–3.
2. T. Tani, T. Suzumoto and K. Ohzeki, *J. Phys. Chem.* **94,** 1298 (1990).
3. J. E. Maskasky, *Langmuir* **7,** 407 (1991); *J. Imaging Sci.* **35,** 29 (1991).
4. H. Saijyo, T. Issiki, M. Shiojiri, H. Ohtani, G. Ning, and K. Ogawa, *J. Imaging Sci.* **37,** 348 (1993).
5. M. Kawasaki and H. Ishii, *J. Imaging Sci.* **39,** 210 (1995).
6. H. Asanuma and T. Tani, *J.Phys. Chem. B* **101,** 2149 (1997).
7. H. Mifune, *J. Soc. Photogr. Sci. Technol. Jpn* **60,** 320 (1997).